

UNCLASSIFIED

Defense Technical Information Center  
Compilation Part Notice

ADP010730

TITLE: DLR Cavity Pressure Oscillations,  
Experimental

DISTRIBUTION: Approved for public release, distribution unlimited

This paper is part of the following report:

TITLE: Verification and Validation Data for  
Computational Unsteady Aerodynamics [Donnees de  
verification et de valadation pour  
l'aerodynamique instationnaire numerique]

To order the complete compilation report, use: ADA390566

The component part is provided here to allow users access to individually authored sections of proceedings, annals, symposia, ect. However, the component should be considered within the context of the overall compilation report and not as a stand-alone technical report.

The following component part numbers comprise the compilation report:

ADP010704 thru ADP010735

UNCLASSIFIED

## 21E. DLR CAVITY PRESSURE OSCILLATIONS, EXPERIMENTAL

Jan Delfs  
 Institute of Design Aerodynamics  
 DLR German Aerospace Center  
 Braunschweig  
 Germany

### INTRODUCTION

Windtunnel tests were carried out with the aim of establishing a measured unsteady surface pressure data set in and around a box-shaped shallow cavity, subject to tangential flow in the transonic Mach number range. Apart from the baseline case, for which systematic Mach number and Reynolds number variations were completed, the main purpose of the tests was to investigate the effect of certain upstream mounted passive flow control devices on the cavity oscillations for selected Mach numbers. This chapter contains the description of two baseline case data sets of unsteady surface pressures for freestream Mach number  $M_\infty = 0.8$  and  $M_\infty = 1.33$  respectively, made available to RTO.

The main purpose of the experiment was to test techniques for the passive control of pressure oscillations occurring in and near cavities exposed to tangential transonic flows. Moreover, the phase relation among the different cavity modes were investigated since the design of devices (passive and especially active) for control, critically depends on the knowledge and an understanding of the underlying physical mechanisms responsible for the resonances driving the phenomenon. Despite its long term investigation and the corresponding vast literature on cavity oscillations, reliable prediction schemes exist only for the frequencies of the oscillation modes. An insight into the phase relations among the modes however is necessary e.g. in order to lay out the characteristics of a controller for a closed loop active control of the oscillations. Therefore the present tests were also performed to reveal the spatio-temporal phase relation among the modes in the cavity.

The tests were done in the DLR wind tunnel TWG (Transonic Windtunnel Göttingen) in November 1997. The closed system tunnel has a test section area of 1 m x 1 m and is operated continuously. The cavity oscillation model is mounted on a cropped sting and consists basically of a flat plate, containing the cutout for the box-shaped cavity of length  $L = 0.202$  m, width  $W = 0.03$  m and depth  $D = 0.05$  m, which in turn is hosted in the fuselage carrying the model (for details of the geometry see section 2 and Figures 1-5). Unsteady surface pressures were measured using flush mounted Kulite pressure transducers as specified in Table 1 and Figures 1 and 5. The static pressures at three positions on the plate surface upstream of the cavity (details see section 7) were measured in order to determine the actual Mach number of the flow above the cavity. A geometrical angle of attack of  $\alpha = 1^\circ$  was set in order to assure non-separating flow at the sharp leading edge of the plate.

The cavity's bottom surface was made of an aluminium plate, which could be translated along the  $x$ -direction (streamwise) with the help of a remote-controlled electric motor. Six equally (in  $x$ ) spaced Kulite sensors were flush mounted into the moveable plate. It was possible to take measurements at arbitrary  $x$ -positions of the cavity's bottom surface by moving the plate (and thus the six sensors) to the desired setting. For each flow parameter this was done for 12 positions of the plate. From one position to the next, the plate was advanced upstream in steps of 3 mm. For each of these settings the time histories of all Kulite sensors (including all non-moveable sensors) were recorded simultaneously along with the static flow data. Thus for each of the 12 positions the phase relation between all sensors can be evaluated.

### LIST OF SYMBOLS AND DEFINITIONS

D	depth of cavity (50.0 mm)
L	length of cavity (202.0 mm)
W	width of cavity (30.0 mm)
$M_\infty$	freestream Mach number
$\alpha$	angle of attack, degrees
$\beta$	angle of sideslip, degrees
$T_0$	stagnation temperature, K

### FORMULARY

#### 1 General description of model

1.1 Designation	COM TWG 1
1.2 Type	empty cavity
1.3 Derivation	model manufactured at DLR Braunschweig central workshop
1.4 Additional remarks	none
1.5 References	none

#### 2 Model geometry

2.1 Planform	rectangular shallow cavity in flat rectangular plate with triangular $50^\circ$ side ears, plate width 300 mm
2.2 Cavity dimensions	length: 202 mm, width: 30 mm, depth: 50 mm

2.3 Leading edge sweep	cavity: 0°, plate: 0° inner i.e., 50° outer i.e.
2.4 Trailing edge sweep	cavity: 0°, plate: 50°
2.5 Taper ratio	n/a
2.6 Twist	0°
2.7 Root chord	plate root chord: 620 mm
2.8 Span of model	plate span : 700 mm
2.9 Area of planform	n/a
2.10 Definition of profiles	symmetrical flat plate with sharp 5°-leading and 20°-trailing edges, plate thickness 10 mm, cavity's leading edge 250 mm downstream of leading edge of plate
2.11 Additional remarks	dihedral = 0°; full geometry in attached figures.
2.12 References	none
<b>3 Wind tunnel</b>	
3.1 Designation	DLR Transonic Wind Tunnel Göttingen, Germany
3.2 Type of tunnel	continuous flow
3.3 Test section dimensions	closed section: height: 1.00 m, width: 1.00 m
3.4 Type of roof and floor	smooth ( $1.3 \leq M_{\infty} \leq 2.2$ ), perforated ( $0.5 \leq M_{\infty} \leq 1.2$ )
3.5 Type of side walls	like roof and floor
3.6 Ventilation geometry	perforated test section: 60° inclined 10 mm holes, 5.8% opening ratio
3.7 Thickness of side wall boundary layer	at test position: 70mm ( $M_{\infty} = 0.5$ ), 59mm ( $M_{\infty} = 0.9$ ), 39mm ( $M_{\infty} = 1.2$ ), 38mm ( $M_{\infty} > 1.3$ )
3.8 Thickness of boundary layers at roof and floor	like side walls
3.9 Method of measuring velocity	perforated test section: calibrated function of plenum to total pressure, laval test section: calibrated laval nozzle
3.10 Flow angularity	perforated test section: $\Delta\alpha, \Delta\beta < 0.03^\circ$ , laval test section: $\Delta\alpha < 0.1^\circ, \Delta\beta < 0.05^\circ$
3.11 Uniformity of Mach number over test section	$\Delta v/v < 0.1 \%$
3.12 Sources and levels of noise in empty tunnel	no specs
3.13 Tunnel resonances	no evidence of resonance in tests
3.14 Additional remarks	accuracy of Mach number $\Delta M_{\infty} < 0.001$ ( $M_{\infty} \leq 0.9$ ), $\Delta M_{\infty} < 0.005$ ( $M_{\infty} > 0.9$ )
3.15 References on tunnel	1
<b>4 Model motion</b>	
4.1 General description	no motion
4.2 Natural frequencies and normal modes of model and support system	response to momentarily released load in vertical direction (z) revealed only one dominant eigenfrequency of $f = 12.5$ Hz of a bending mode (no interferences with cavity oscillations)
<b>5 Test conditions</b>	
5.1 Model plan-form area/tunnel area	0.305 (based upon cross section of test section)
5.2 Model span/tunnel width	0.7
5.3 Blockage	2.36% (frontal blockage, including sting interface)
5.4 Position of model in tunnel	plane of plate 50 mm above center of test section, cavity leading edge in streamwise center of test section
5.5 Range of Mach numbers	0.7, 1.46 (freestream)
5.6 Range of tunnel total pressure	$0.79 \cdot 10^5$ Pa ( $M_{\infty} = 1.33$ ), $0.82 \cdot 10^5$ Pa ( $M_{\infty} = 0.8$ )
5.7 Range of tunnel total temperature	$300 \text{ K} < T_0 < 320 \text{ K}$
5.8 Range of model steady, or mean incidence	$-1.0^\circ < \alpha < 0^\circ, \beta = 0$
5.9 Definition of model incidence	model incidence defined relative to the plate's plane
5.10 Position of transition, if free	not measured
5.11 Position and type of trip, if transition fixed	no tripping

5.12 Flow instabilities during tests	cavity oscillations
5.13 Changes to mean shape of model due to steady aerodynamic load	not measured, negligible
5.14 Additional remarks	boundary layer thickness at leading edge $x = l_{LE} = 250$ mm of cavity not measured; estimated to be about 4.4 mm for both considered cases (estimation based upon transition from laminar to turbulent boundary layer at $Re_{Tr} = 3.5 \cdot 10^5$ )
5.15 References describing tests	none
<b>6 Measurements and observations</b>	
6.1 Steady pressures for the mean conditions	yes, freestream values (wind tunnel) and 3 pressure taps in plate upstream of cavity
6.2 Steady pressures for small changes from the mean conditions	no
6.3 Quasi-steady pressures	no
6.4 Unsteady pressures	yes, KULITE pressure sensors in front, behind and in the cavity
6.5 Steady section forces for the mean conditions by integration of pressures	no
6.6 Steady section forces for small changes from the mean conditions by integration	no
6.7 Quasi-steady section forces by integration	no
6.8 Unsteady section forces by integration	no
6.9 Measurement of actual motion at points on model	no
6.10 Observation of measurement of boundary-layer properties	no
6.11 Visualisation of surface flow	no
6.12 Visualisation of shock wave movements	high speed schlieren movie to visualize sound radiation from cavity
6.13 Additional remarks	accuracy of floor plate sliding mechanism: $\pm 0.15$ mm
<b>7 Instrumentation</b>	
7.1 Steady pressures	
7.1.1 Position of orifices span-wise and chord-wise	P1 ( $x = 50$ mm, $y = 0$ mm, $z = 0$ mm), P2 ( $x = 100$ mm, $y = 0$ mm, $z = 0$ mm), P3 ( $x = 120$ mm, $y = 0$ mm, $z = 0$ mm), see also Fig.1
7.1.2 Type of measuring system	pressure orifices in model surfaces. connected to PSI pressure measurement system
7.2 Unsteady pressures	
7.2.1 Position of orifices span-wise and chord-wise	see Fig. 5 and Tab. 1
7.2.2 Diameter of orifices	transducers flush mounted
7.2.3 Type of measuring system	PSI modules, KULITE pressure transducers
7.2.4 Type of transducers	KULITE pressure transducers LQ3A-064-25A having 3.14 mm diameter
7.2.5 Principle and accuracy of calibration	PSI: 3 calibration pressures (magnitudes adapted to the expected values of the experiment) applied to each module. Kulite: static calibration at beginning of tunnel entry
7.3 Model motion	
7.3.1 Method of measuring motion reference coordinate	N/A
7.3.2 Method of determining spatial mode of motion	N/A
7.3.3 Accuracy of measured motions	N/A
7.4 Processing of unsteady measurements	
7.4.1 Method of acquiring and processing measurements	amplified Kulite signals input to DLR DEAS data acquisition system. Data sampling rate 30 kHz for 0.25 s simultaneously for all Kulites, repeated for 12 positions of the set of 6 Kulites, fixed to the translateable floor plate of cavity, translations in steps of 3 mm

7.4.2 Type of analysis	none
7.4.3 Unsteady pressure quantities obtained and accuracies achieved	time history data
7.4.4 Method of integration to obtain forces	N/A
7.5 Additional remarks	no mean pressure information from Kulite-signals
7.6 References on techniques	none

## 8 Data presentation

8.1 Test cases for which data could be made available	$0.7 \leq M_{\infty} \leq 1.2$ in steps of $\Delta M_{\infty} = 0.05$ (except $M_{\infty} = 1.0$ ) for $Re(0.1 \text{ m}) = 1.7 \cdot 10^6$ $M_{\infty} = 0.8, 1.2, 1.33, 1.41, 1.46$ for $Re(0.1 \text{ m}) = 1.1 \cdot 10^6$ $M_{\infty} = 0.8, 1.33$ for $Re(0.1 \text{ m}) = 0.55 \cdot 10^6$
8.2 Test cases for which data are included in this document	$M_{\infty} = 0.8, 1.33$ for $Re(0.1 \text{ m}) = 1.1 \cdot 10^6$
8.3 Steady pressures	freestream conditions and data from 3 pressure taps
8.4 Quasi-steady or steady perturbation pressures	N/A
8.5 Unsteady pressures	see above
8.6 Steady forces or moments	N/A
8.7 Quasi-steady or steady perturbation forces	N/A
8.8 Unsteady forces and moments	N/A
8.9 Other forms in which data could be made available	none
8.10 References giving other presentation of data	none

## 9 Comments on data

9.1 Accuracy	
9.1.1 Mach number	see 3.14
9.1.2 Steady incidence	$-1^{\circ}$
9.1.3 Reduced frequency	N/A
9.1.4 Steady pressure coefficients	N/A
9.1.5 Steady pressure derivatives	N/A
9.1.6 Unsteady pressure coefficients	N/A
9.2 Sensitivity to small changes of parameter	no evidence
9.3 Non-linearities	N/A
9.4 Influence of tunnel total pressure	indirect effect through Reynolds number
9.5 Effects on data of uncertainty, or variation, in mode of model motion	N/A
9.6 Wall interference corrections	none
9.7 Other relevant tests on same model	none
9.8 Relevant tests on other models of nominally the same shapes	none
9.9 Any remarks relevant to comparison between experiment and theory	the tests were not performed as dedicated validation experiments for CFD/CAA (Computational Aeroacoustics), but were used to show that some new concepts of reducing cavity pressure oscillations were indeed able to destroy the resonances. Special flow devices were installed upstream the cavity to modify favourably the aerodynamic properties of the cavity shear layer. The devices were able to act in a way as to not increase the broadband level of the pressure oscillations
9.10 Additional remarks	none
9.11 References on discussion of data	none

## Personal contact for further information

Dr. Jan Delfs  
DLR, Institut für Entwurfsaerodynamik  
Lilienthalplatz 7  
38108 Braunschweig, Germany  
jan.delfs@dlr.de

## List of references

- Binder, B; Riethmüller, L; Tuschke, S.; Wulf, R.; Modernisierung des Transsonischen Windkanals in Göttingen. DGLR Jahrbuch 1992 Band1, pp 37-249

## FORMAT OF DATA SET

There exists one ASCII data file for each position of the bottom plate of the cavity, in correspondence with the recording of the experimental data. The position is given and identified by a designation, which is a number  $i = 0, \dots, 11$  with the following meaning: The position of the plate is called  $i$ , when the  $x$ -position of plate-mounted sensor 8 is at  $x_8 = (285.0 - i \cdot 3)$  mm. The mean position of sensor 8 is indicated in Table 1 and Figure 5. The position  $i$  is also indicated in the header of each of the files as well as in the name of the respective file. The data files of the two mentioned test cases ( $M_\infty = 0.8$  and  $M_\infty = 1.33$ ) are given as 080\_0i.dat or 133\_0i.dat for  $i < 9$  and 080\_i.dat or 133\_i.dat for  $i > 9$ . All mean flow data defining the case considered are given in the header of each file. All data are given in SI-units. The sampling rate of the unsteady pressure data was 30 kHz for all cases. The corresponding time history of all 18 Kulite sensors is listed in the form of 18 respective columns in each of the mentioned data files. The files are compressed using the Unix command `compress`, i.e. they appear with an additional extension ".Z".

It is emphasized that the Mach number and the dynamic pressure of the flow above the cavity are slightly different from the specified freestream values. The true values are to be computed from the standard oblique shock relations, taking into account the measured static pressures at the pressure taps.

It is noted, that in the case  $M_\infty = 0.8$  the positions  $i = 0, 1, 2$  are missing, because of a defect of the sliding mechanism of the cavity's bottom plate. Moreover, for the same Mach number the Kulite sensor No. 6 gave incorrect data. In the case  $M_\infty = 1.33$  the signal from Kulite sensor No. 3 is incorrect (the signals of No. 6 being correct). All further details of the experiments are given in sections 1-12. The first lines of a sample data file are printed below. The columns corresponding to Kulites 4 to 17 are omitted in the sample.

```
# cavity oscillation experiment, DLR COMTWG1
#
# 0.800000 E+00      freestream Mach number
# 1.043000 E+06      Reynolds number Re (0.1m)
# 1.000000 E+00      angle of attack (in degree)
# 0.817914 E+05      total pressure in [Pa]
# 3.113927 E+02      stagnation temperature in [K]
# 5.370493 E+04      static pressure tap1 in [Pa]
# 5.378215 E+04      static pressure tap2 in [Pa]
# 5.428271 E+04      static pressure tap3 in [Pa]
# 3.000000 E+04      temporal sampling rate in [s^-1]
# 3                  number of position of translatable plate
# p1                p2                p3                ...                p18                p19
.64695008E+03      -.77032927E+03      -.79613503E+03      ...                -.10798857E+04      -.11891270E+04
.42323837E+03      -.10607813E+04      -.97915458E+03      ...                -.11894393E+04      -.10731146E+04
.22371171E+03      -.13680711E+04      -.13695963E+04      ...                -.15838324E+04      -.15168620E+04
-.47765473E+03      -.12572223E+04      -.12628349E+04      ...                -.14492379E+04      -.20911233E+04
-.32045191E+03      -.86854976E+03      -.81443698E+03      ...                -.17027763E+04      -.21389784E+04
```

## TABLES

Kulite no.	$x$ [mm]	$y$ [mm]	$z$ [mm]
1	246.5	0.0	0.0
2	250.0	0.0	-5.5
3	250.0	0.0	-11.5
4	250.0	0.0	-17.5
5	250.0	0.0	-23.5
6	250.0	0.0	-29.5
7 not exist.	-	-	-
8	268.5±16.5	0.0	-50.0
9	301.5±16.5	0.0	-50.0
10	334.5±16.5	0.0	-50.0
11	367.5±16.5	0.0	-50.0
12	400.5±16.5	0.0	-50.0
13	433.5±16.5	0.0	-50.0
14	455.5	0.0	0.0
15	452.0	0.0	-5.5
16	452.0	0.0	-11.5
17	452.0	0.0	-17.5
18	351.0	15.0	-17.5
19	351.0	-15.0	-17.5

**Table 1: Positions of Kulite sensors. Kulites 8-13 are mounted on a motor-driven translatable plate, such that any position along the cavity floor can be measured. In the given set of data, the plate was moved in steps of  $\Delta x = 3$  mm.**

FIGURES

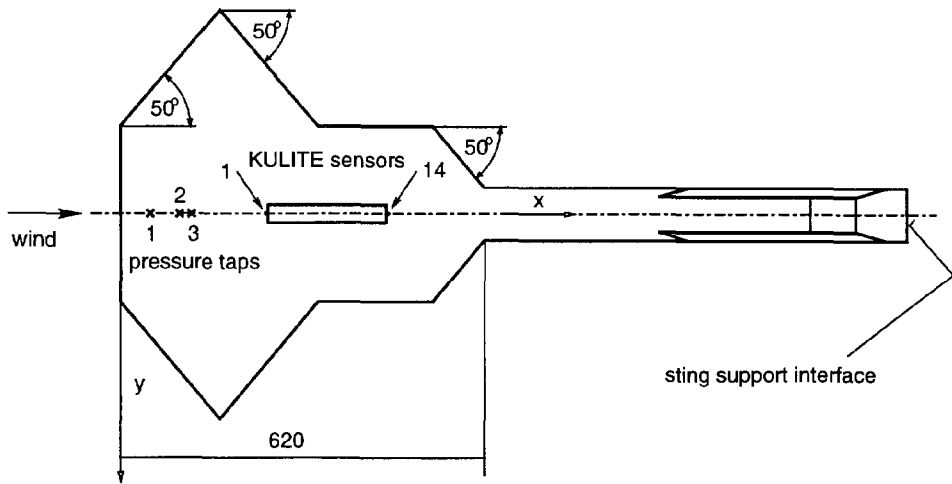


Figure 1: Lower side of model, housing the cavity; position and number of pressure taps and KULITE sensors

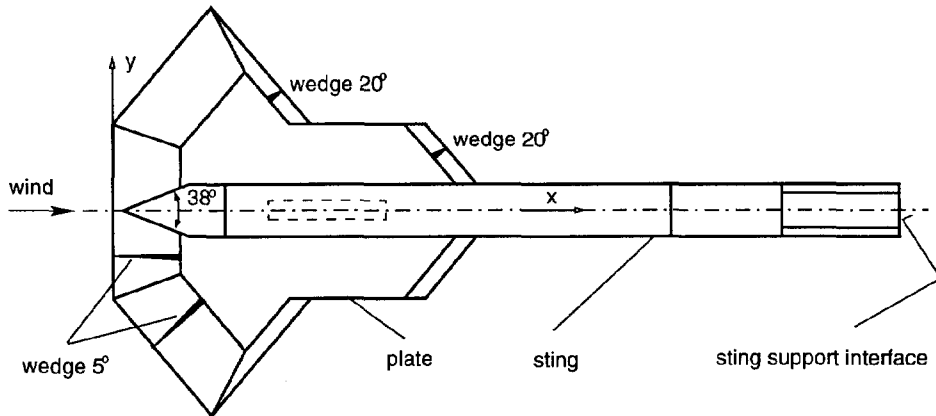


Figure 2: Upper side of the model

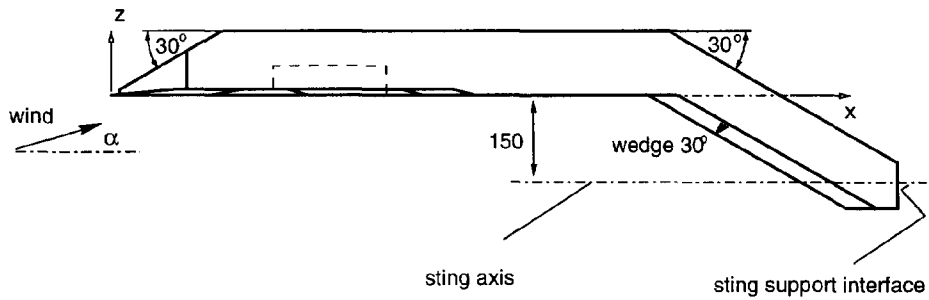


Figure 3: Side view of the model

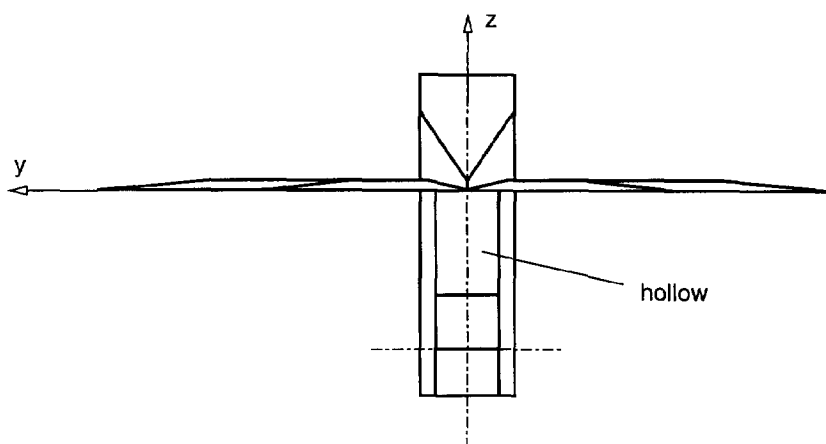


Figure 4: Front view of the model

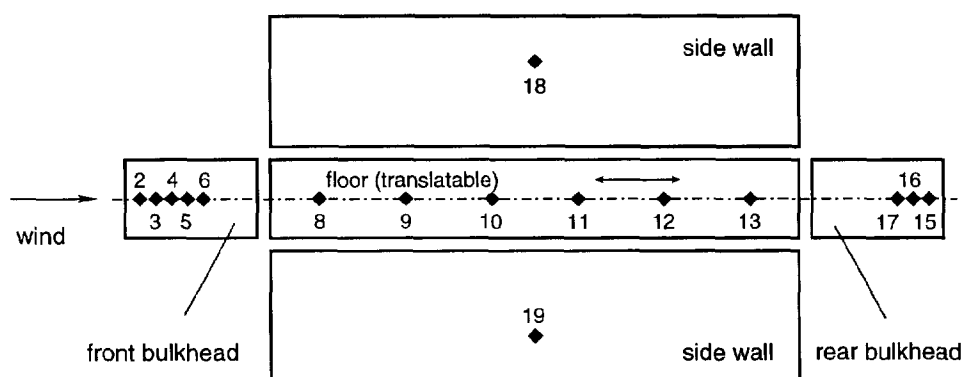


Figure 5: Arrangement and numbering of KULITE sensors on cavity walls

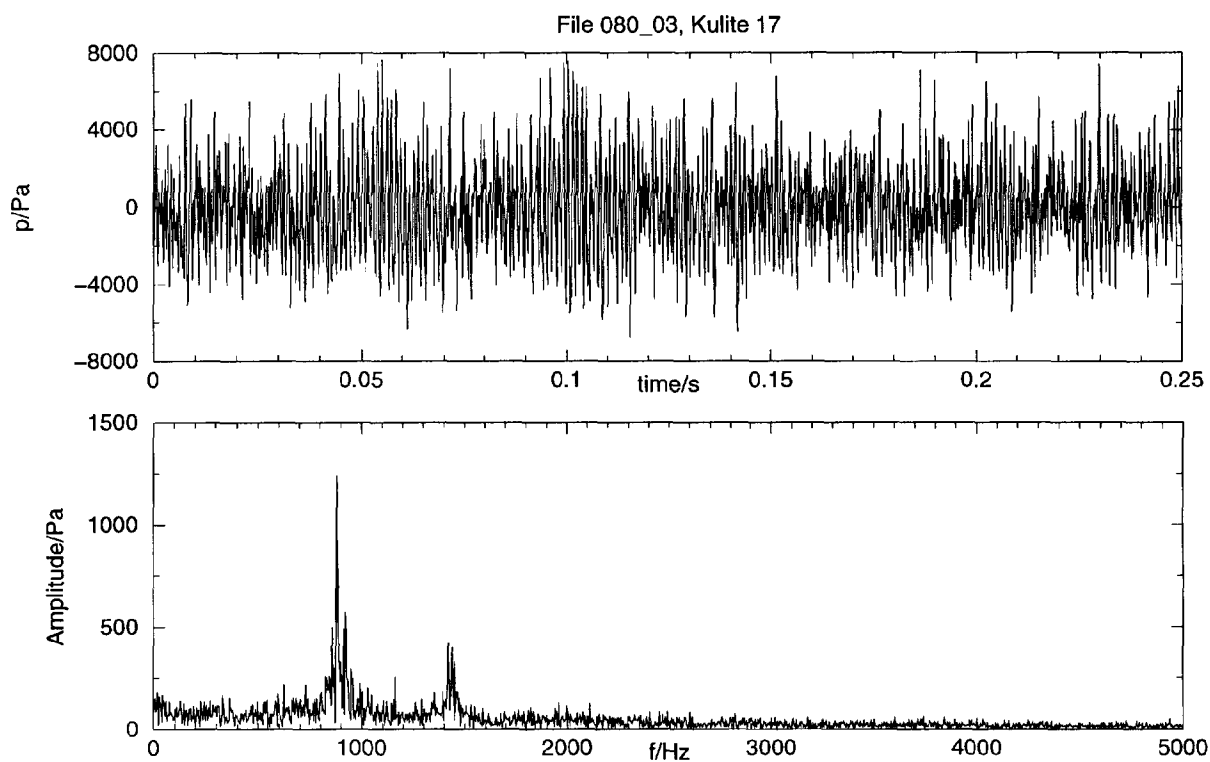


Figure 6: Typical time series and corresponding amplitude spectrum of non-averaged narrow-band Fourier coefficients of Kulite signal

